Evaluation of the repartition of the particles in Pickering emulsions in relation with their rheological properties

Santiago F. Velandia, Philippe Marchal, Cécile Lemaitre, Véronique Sadtler, Thibault Roques-Carmes

Version of Record: https://www.sciencedirect.com/science/article/pii/S0021979721000084
Manuscript_b691fd41ebee6f8094f0d7605824efb5

Evaluation of the repartition of the particles in Pickering emulsions in relation with their rheological properties

Santiago F. Velandia, Philippe Marchal, Cécile Lemaitre, Véronique Sadtler, Thibault Roques-Carmes*

Laboratoire Réactions et Génie des Procédés, UMR 7274 CNRS, Université de Lorraine, 1 rue Grandville, 54001 Nancy, France

santiago-felipe.velandia-rodriguez@univ-lorraine.fr; philippe.marchal@univ-lorraine.fr; cecile.lemaitre@univ-lorraine.fr; veronique.sadtler@univ-lorraine.fr; thibault.roques-carmes@univ-lorraine.fr

(*) corresponding author: Thibault Roques-Carmes: thibault.roques-carmes@univ-lorraine.fr, Tel.: +33 (0)3 72 74 38 33

ABSTRACT

Hypothesis: The distribution of particles in Pickering emulsions can be estimated through a percolation-type approach coupled to the evolution of their rheological features with the dispersed phase volume fraction ϕ.

Experiments: The rheological behavior of water-in-dodecane Pickering emulsions stabilized with hydrophobic silica nanoparticles is addressed. The emulsions viscosity and elastic modulus are investigated at ϕ varying from 0.1 to 0.75. Various rheological models are adjusted to the experimental data.

Findings: The comparison of the elastic modulus evolution of the Pickering emulsions with those of emulsions stabilized with surfactants confirms a major contribution of the particles to the rheological behavior of Pickering emulsions and supports the existence of a three-dimensional network between the droplets. The applied percolation approach allows to quantitively estimate a nanoparticles viscoelastic link between the droplets and opposes the classic vision of interfacial monolayers stabilizing the Pickering emulsions. This network of interconnected particles and droplets contributes significantly to the viscosity as well as the elastic modulus of these emulsions. To our knowledge, the applied percolation-based model is the only one capable of providing a structural explanation while describing the abrupt viscosity and elastic modulus growth of Pickering emulsions across the range of ϕ.

KEYWORDS Pickering; W/O Emulsions; Rheology; Dispersed phase volume fraction; Nanoparticles

1. Introduction

Pickering emulsions are emulsions stabilized by nano or microparticles [1,2]. The large desorption energy of the particles at the oil/water interfaces leads to high kinetic stability of these dispersed systems, mainly, against droplets coalescence [3,4]. Pickering emulsions appear then very attractive for various applications as an alternative to classical emulsions stabilized with surfactants [5,6]. They are increasingly used for the development of innovative products, particularly based on the nature of the particles used (bio-based particles, polymeric particles, biodegradable particles, …) [7,8]. Pickering emulsions may also be produced, under certain circumstances, due to the presence of particles in the system, as is the case of the enhanced oil recovery processes by the injection of viscosifying fluid containing surfactants [9,10].

Two main stabilization mechanisms are generally proposed for these liquid/liquid/particles systems [11-13]. The first is due to the adsorption of particles at oil/water interfaces [14-17]. The particle monolayer or densely packed particle layers produce a rigid film that creates a mechanical barrier against coalescence [16,18]. The second mechanism is based on particle-particle interactions leading to the formation of a 3-dimensional network of particles in the continuous phase [17,19]. This kind of network was already reported with clay-based [14,20] and silica-based systems [15,21]. The formation of a viscoelastic network of particles in the continuous phase generates a significant stability against coalescence by keeping separated droplets and hindering their contact. The interactions of the particles in the continuous phase are decisive for the network formation [20]. When attractive interactions between particles take place, a 3D network formation can be favored leading, in certain cases, to the formation of gels. On the opposite, when repulsive interactions between the particles occur, instead of a network formation, the particles tend to adsorb at the oil/water interfaces [16,20]. It appears also that the 3D network formation is facilitated with high dispersed phase fractions when

particle aggregates extend into the thin film of the continuous phase and trap the droplets within the gel matrix [22].

The rheological analysis appears as one of the most relevant tools for the characterization of emulsions [23]. The rheological properties can be related to the stability and the microstructure of the emulsions. As an example, the yield stress value indicates how well the emulsion can resist to sedimentation or creaming [24]. The rheological measurements can be also employed to investigate the interactions between the particle-stabilized droplets as well as the particulate network formed in the continuous phase through the values of emulsion plateau elastic modulus, yield stress, and shear viscosity.

The dispersed phase volume fraction (ϕ) is a major parameter that conditions the rheological behavior of emulsions. For classical emulsions stabilized by surfactants, the viscosity increases abruptly with ϕ up to a critical fraction which corresponds generally to the random close packing volume fraction of the droplets commonly defined at $\phi = 0.64$ [25-27]. Above this critical fraction, the emulsions present deformation of the interfaces favoring a hexagonal packing, which results in an increase in the elasticity of the systems. Several models have been developed to represent the viscosities and elastic modulus of these emulsions as a function of the dispersed phase volume fraction, the interfacial tension and the droplet diameter [28,29]. For instance, the Princen model accounts fairly well for the experimental data for very large dispersed phase fractions and concentrated emulsions [28,30]. However, it does not work efficiently for all the systems, mainly when a very steep increase of G' with ϕ takes place [30]. Recently, we have applied a percolation approach which represents satisfactorily the evolution of both the viscosity and elasticity with ϕ [31]. For Pickering emulsions, less experimental data are available, and only one model has been developed to describe the evolution of the viscosity with ϕ [32]. To our knowledge, no model has been developed and tested for the elastic modulus of Pickering emulsions. There is also a

need to test the models elaborated for classical emulsions, the ones mentioned above but also others, with particles stabilized emulsions.

In this paper, the rheological behavior of Pickering emulsions from the dilute to the concentrated domain is addressed. Water-in-dodecane emulsions stabilized with hydrophobic silica nanoparticles are used as a W/O Pickering emulsion model system. Shear viscosity and elastic modulus of emulsions are characterized. A phenomenological model based on percolation theory is fitted to the experimental points and compared to other existing models for Pickering emulsions and surfactant stabilized emulsions. Furthermore, the rheological study coupled to percolation theory highlight new understanding of the repartition of the particles in Pickering emulsions.

2. Materials and methods

2.1. Materials

Reverse (W/O) Pickering emulsions were prepared by mixing milli-Q filtrated and de-ionized water (18 MΩ cm resistivity), sodium chloride (BioXtra ≥ 99.5%), dodecane (ReagentPlus ® ≥ 99%, density 0.75 g/mL at 25 °C, dynamic viscosity 1.380 mPa s at 25 °C), and silica nanoparticles. Aerosil® R-972 (specific area 110 ± 20 m^2/g, particle size dp = 16 nm, contact angle 114° [33]) was kindly provided by Evonik (Germany). This fumed silica was mainly hydrophobic due to the methylation of 70% of the hydroxyl surface groups. Aerosil® R-972 silica nanoparticles, as well as the other materials mentioned before, were used without any further treatment. The total mass of emulsion prepared for every sample was 18 g.

2.2. Preparation of emulsions

The emulsion preparation was performed similarly to a semi-batch process following a three-step protocol reported in the literature [34]. First, the dispersed and continuous phases

were prepared independently. Sodium chloride was dissolved in water at a concentration λ of 1 wt.%. In order to break up as many agglomerates as possible, as well as to ensure homogeneous dispersion of nanoparticles, ultrasounds are often used. In the present study, the oily phase was prepared by dispersing the desired silica nanoparticles quantity (ε = 1 wt.% relatively to the total amount of water dispersed phase in the O/W emulsion) with an ultrasonic process (Sonic Dismembrator 550-Fisher Scientific-20 kHz frequency-standard probe). The time of exposure to ultrasounds was 90 s (pulse on 2s-pulse off 2s) at an amplitude of 70%. An ice bath was used to control temperature increase. Secondly, the dispersed phase was added progressively to the oil phase using a peristaltic pump (BVP-Ismatec) with a flow rate of 5.2 mL min^{-1}. This stage was performed under agitation with an Ultra-Turrax turbine blender (IKA T25 Basic / Dispersion Tool S25-NK-19G, Germany) at a rate of 13500 rpm for an average time of 2 min.

Note that a flow rate of 5.2 mL min^{-1} corresponded to a flow rate of less than 0.1 mL s^{-1}. This value was approximately equivalent to those used when the dispersed phase was added dropwise to a continuous phase without a fixed flow rate. Finally, the emulsion was homogenized by stirring for 3 min, maintaining the same operating conditions as for the previous stage. Throughout this last stage, the Ultra-Turrax head was moved from bottom to top to counteract local dead zones during the agitation process. The temperature was kept constant at 25 °C during all the process. Special attention was given to the dispersed phase volume fraction of emulsions (ϕ) which was varied between 0.1 and 0.75. Note also that, under the present preparation conditions, no emulsion could be produced for water dispersed volume fractions larger than 0.75.

The silica content can be compared to the mass of particles needed to form a monolayer at the interface of all the droplets (m_p). To estimate m_p, the approach of Arditty et al. was used [35]. This model assumes that all the particles are adsorbed at the oil/water interfaces. It also

considers that the particles are spherical and that the contact angle at the water-particle-oil interface reaches 90°. At the same time, the particles are assumed to adopt the maximum geometric coverage at the interface. This means that a hexagonal organization of the droplets takes place at the interface. In other words, a monolayer of hexagonally packed particle is anchored at the surface of the droplets. Under these conditions, the surface coverage parameter *C*, which is the ratio of the total area that may be covered by the particles over the total interfacial area, is equal to 0.9. The mass of particles needed to form a monolayer at the interface of all the droplets can be estimated as [11,35]:

$$m_p = \frac{4C\rho_p d_p V_d}{D} \quad (1)$$

where ρ_p is the particle density, D is the droplet diameter, V_d is the volume of the dispersed phase, and d_p is the particle diameter.

The calculated values of m_p for all the prepared emulsions are reported in Table S1 of the Supporting Information. The corresponding theoretical mass fraction corresponding to a monolayer ($\varepsilon_{monolayer} = m_p/m_d$), where m_d is the mass of the disperse phase, can be compared to the mass fraction of silica introduced in the emulsion ($\varepsilon = m_{silica}/m_d$). We estimated a minimal required particle concentration of $\varepsilon_{monolayer}$ = 0.42 wt.% to ensure a complete coverage of droplets for all the configurations. This implies that all formulations were "overloaded" with nanoparticles since all the emulsions exhibited ε = 1 wt.%. Note that this minimal value is consistent with the impossibility in the present study to produce emulsions at silica concentrations lower than 0.5 wt.%.

Dilution experiments and conductivity measurements were constantly performed in order to verify the type of emulsion (W/O or O/W).

2.3. General aspects of Pickering W/O emulsions prepared

All the formulated Pickering systems presented the ability to be diluted in dodecane and exhibited conductivity values lower than 10^{-5} S cm^{-1}, which confirmed the presence of reverse W/O emulsions. Fig. 1 shows microscopic images of W/O Pickering emulsions at various dispersive phase fractions. W/O systems were polydisperse. For dispersed phase fraction of 0.75, the droplets showed polyhedral shapes as a consequence of close packing. No phase inversion was identified in the range of the studied dispersed phase volume fractions (ϕ = 0.1 - 0.75).

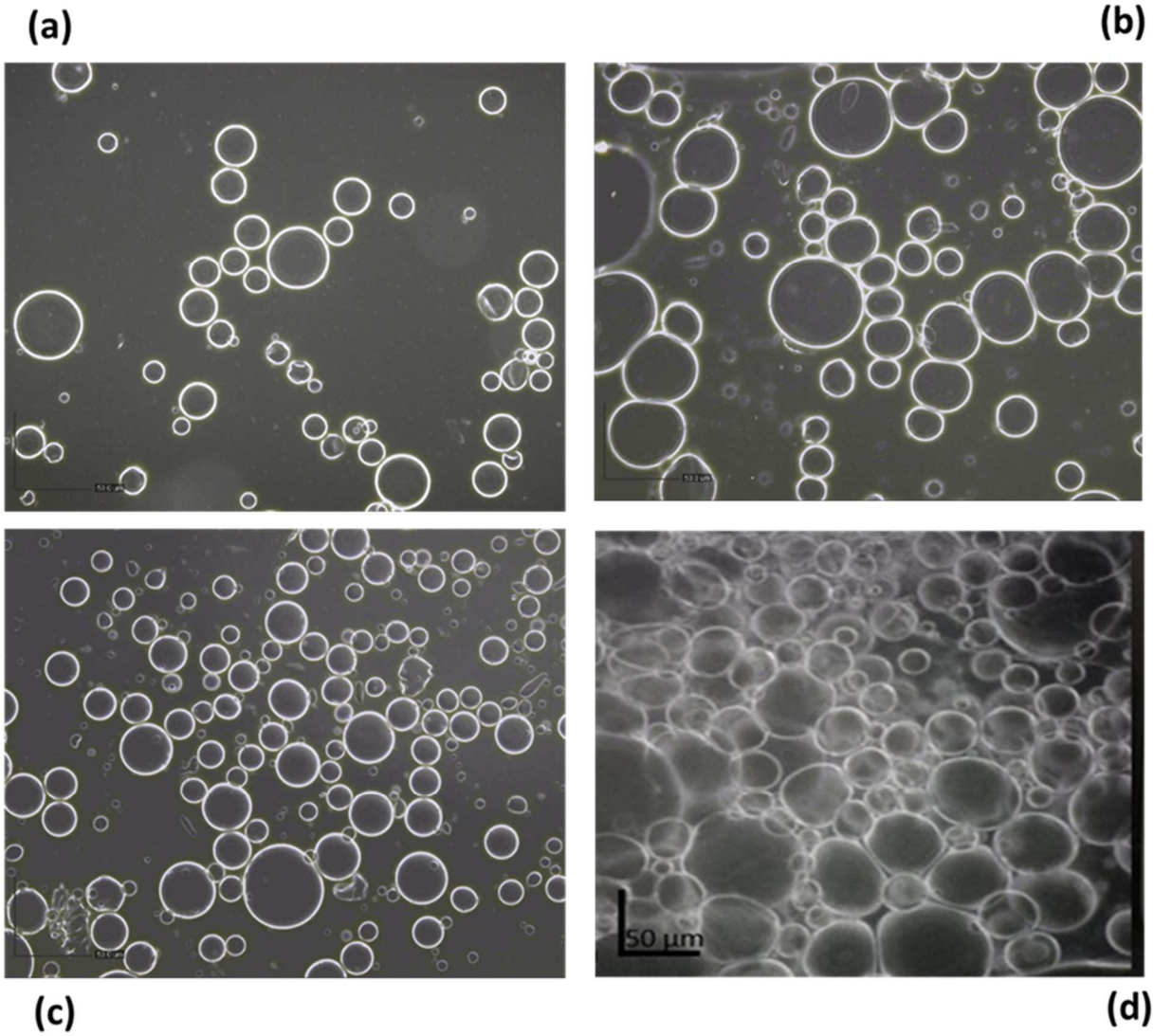

Fig. 1. Microscopic images of W/O emulsions. Dispersed phase fraction of water of (a) ϕ = 0.10, (b) ϕ = 0.40, (c) ϕ = 0.50, and (d) ϕ = 0.75. Silica content ε = 1 wt.%, NaCl concentration λ = 1 wt.%.

Considering limitations associated with dynamic light scattering techniques for Pickering W/O emulsions, such as nanoparticle interferences and the need for large quantities of dodecane (for the emulsion dilution step), optical microscopy and image processing were chosen to estimate the droplet size distributions. The optical microscope was a digital microscope AM7515MT8A Dino-Lite Edge. For the microscopy observation, a small amount of the emulsions was placed between a bottom glass slide and a cover glass side. For each emulsion, the size of at least 400 droplets was measured. Fig. 2 presents droplet size distributions for different dispersed phase volume fractions.

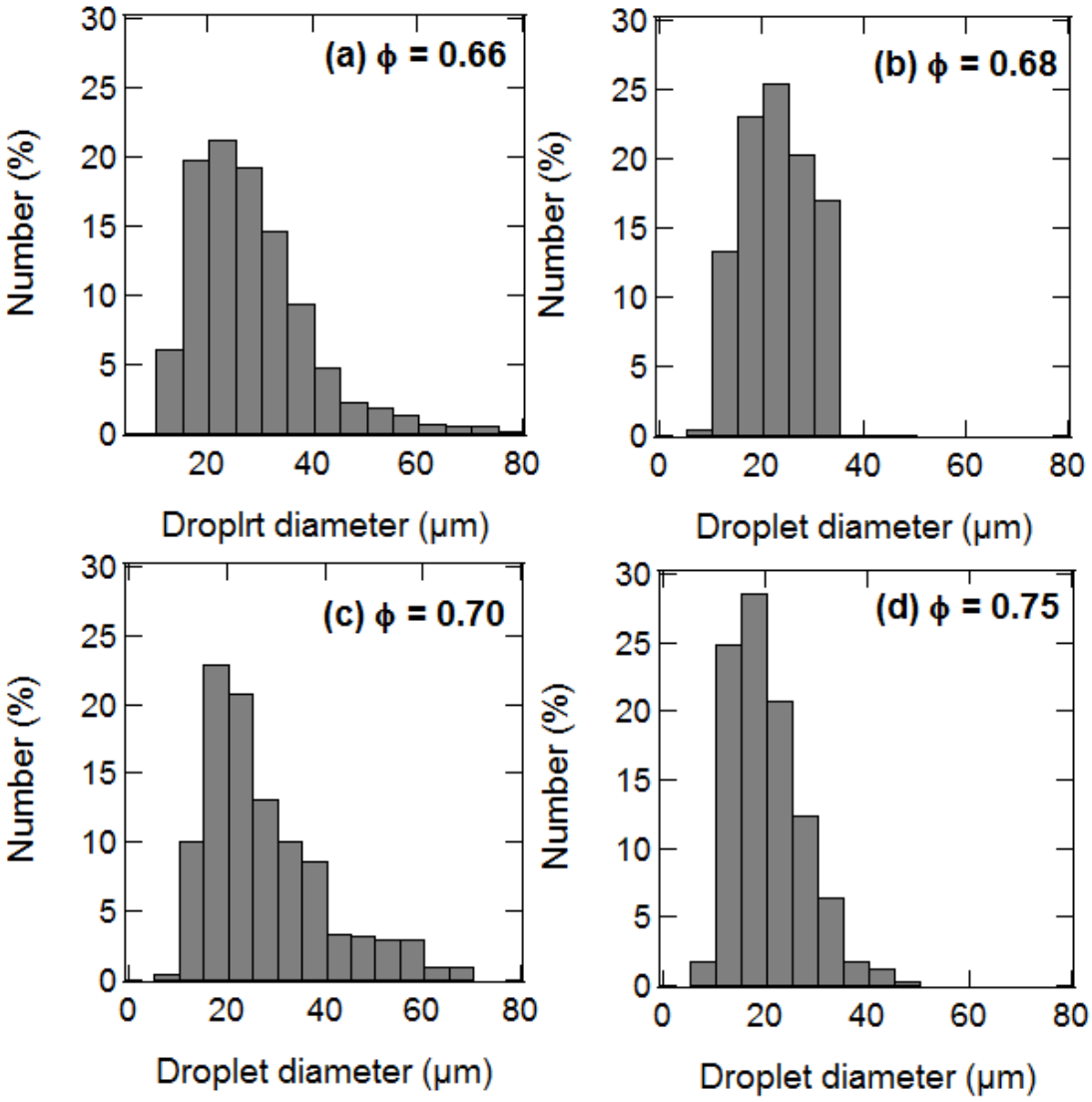

Fig. 2. Droplet diameter distribution of W/O emulsions prepared at dispersed phase volume fractions (ϕ) of (a) 0.66, (b) 0.68, (c) 0.70 and (d) 0.75.

All the prepared emulsions resulted to be polydisperse with droplets size distribution ranging from 10 to 60 μm. However, the average diameter of the droplets diminishes with the dispersed water volume fraction. This behavior corresponds well with previously published results since the general trend reported in the literature is to obtain a decrease of the droplet sizes with the increase of the dispersed phase fractions [36-40]. The improvement of the dispersed phase fraction produces an increase of the viscosity and the shearing of the droplets becomes more efficient [39,40].

2.4. Rheological characterization

The rheology of Pickering W/O emulsions was studied with an ARES Rheometer from TA instruments. It was a strain-imposed rheometer. All the rheological experiments were carried out with a fresh emulsion just after preparation. The W/O emulsions were gently stirred by hand just before their rheological characterization to allow homogenization of the samples without altering their structure. For all samples, measurements were performed using a titanium parallel plate geometry with a diameter of 25 mm and a gap of 1 mm, at a temperature of 20 °C. Flow and oscillatory tests were carried out to characterize hydrodynamic (viscosity) and structural (elastic moduli) characteristic properties of Pickering systems.

Oscillatory strain sweeps were used to identify the linear viscoelastic regions while the shear viscosity was determined through transient step rate measurements. The first type of test was done at the constant frequency of 1 rad/s and a shear strain amplitude increasing from 10^{-4} to 1. In order to study the elastic behavior of emulsions, the storage modulus G' was presented as a function of the shear strain. In the second test type, samples were sheared during four steps of 100 s^{-1}, 30 s^{-1}, 100 s^{-1}, and 10 s^{-1}. This special procedure was used because at very low dispersed volume fractions, the sedimentation of the droplets of waters could occur during the rheological measurements and, then, disturb the test and affect the value of the viscosity. Consequently, before each measurement at a given shear rate, the sample was sheared at a rate of 100 s^{-1} in order to produce the remixing of the emulsion. In addition, the viscosity measured at a shear rate of 100 s^{-1} was also taken as an experimental data. Each step lasted 100 s and the viscosity was reported at 100 s^{-1} to ensure a better measurement sensitivity and to obtain reliable viscosity for all the dispersed volume fractions. As a matter of fact, at low dispersed volume fractions, the viscosities at shear rates of 10 and

30 s^{-1} did not have sufficiently high measurement sensitivity. Each experiment was carried out at least twice to ensure the repeatability of the rheological behavior.

3. Results and discussion

3.1. Influence of the dispersed phase volume fraction

In terms of flow curves (viscosity vs. shear rate), all the emulsions display a shear-thinning rheological behavior (not shown here). In other words, a viscosity decrease for an increasing shear rate is reported. Concerning the oscillatory tests, an example of typical curve showing the evolution of the elastic modulus as a function of the shear strain is displayed in Fig. S1 of the Supporting Information. It is worth mentioning that for all the prepared emulsions, the storage modulus *G'* overcomes the loss modulus *G''* (not shown) whatever the frequencies, shear strain or shear stress applied to the samples. This emphasizes the predominance of the solid-like/elastic behavior of the emulsions. All the curves display the same trend: *G'* remains constant at low shear strain in the linear viscoelastic regime while it decreases at larger shear strain γ. Furthermore, linear viscoelastic regions characterized by the *G'* "plateau" are observed in each diagram. The value extracted from this zone is reported in the G' versus ϕ curves. To evaluate the effect of the water-phase volume fraction, the viscosity and elasticity of the emulsions were plotted as a function of the dispersed phase volume fraction ϕ (Fig. 3). The viscosities reported in the figure were extracted from the flow curves for a shear rate of 100 s^{-1}. Conversely, for the elastic modulus, the values were taken into the linear viscoelastic region.

The figure displays classical behaviors generally encountered in the literature. At low volume fraction, a slight increase of η with ϕ is reported. When the dispersed volume fraction exceeds 0.3, the viscosity increases moderately and then sharply. The *G' vs* ϕ curve follows the same classical trend but is shifted along the ϕ axis. Above a dispersed volume fraction of

0.4, the emulsions acquire elasticity ($G' \neq 0$) which is drastically enhanced for very large dispersed phase volume fractions ($\phi = 0.65–0.75$). In an attempt to describe and explain these behaviors, both qualitatively and quantitatively, it is useful to use models and assess how accurately they describe the experimentally-observed rheological behaviors.

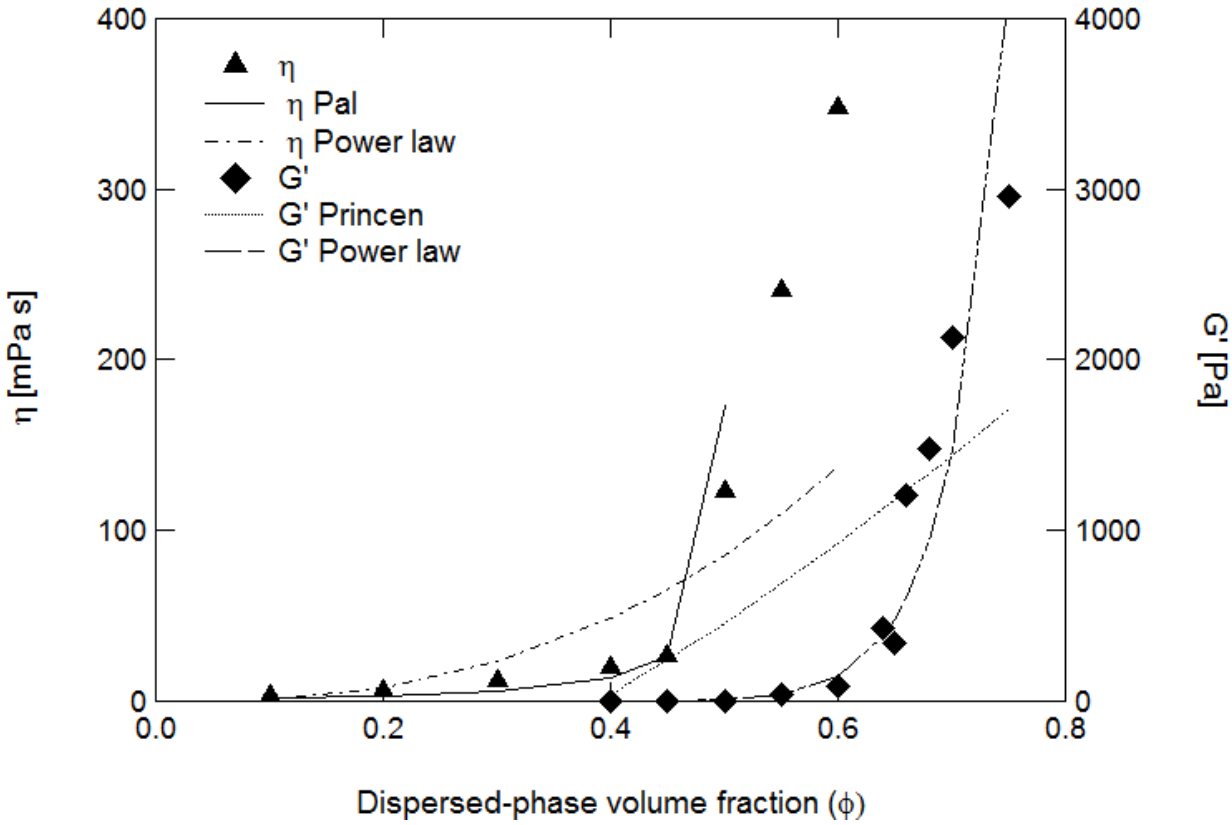

Fig. 3. Shear viscosity η and elastic modulus G' as a function of the dispersed-phase volume fraction ϕ. Comparison of the experimental viscosity data (points, triangles) with those calculated with the Pal approach (Eq. (4)) and those fitted by a power law expression (Eq. (6)). Comparison of the experimental elastic modulus (points, diamonds) with those fitted with the Princen model (Eq. (5)) and those fitted by a power law expression (Eq. (7)).

Pal recently developed a model describing the evolution of the viscosity with the dispersed phase for the special case of Pickering emulsions [32]. In this model, emulsions are considered as dispersions of solid spheres because of the solid-like structure imparted to the

droplets by the particles anchored at the droplet interface as monolayers. More precisely, particle-covered droplets are seen as solid particles with a radius equal to the sum of the droplet radius (R_d) and the diameter (d_p) of particles belonging to the monolayer (Fig. 7b). Then, for each volume fraction of the dispersed phase, it becomes possible to estimate the volume fraction of the core/shell droplets ϕ_s with the relation:

$$\phi_s = \phi\left(1 + \frac{d_p}{R_d}\right)^3 \quad (2)$$

where ϕ is the volume fraction of the bare droplet.

To consider the aggregation of the droplets in Pickering emulsions, the volume fraction of the dispersed phase ϕ_{agg} is expressed as:

$$\phi_{agg} = \phi_s\left(1 + \left(\frac{1-\phi_g}{\phi_g}\right)\sqrt{1 - \left(\frac{\phi_g - \phi_s}{\phi_g}\right)^2}\right) \quad (3)$$

where ϕ_g is the glass transition volume fraction for which the entire emulsion jammed into a single large cluster. Typical values of ϕ_g range between 0.51 and 0.58 [32]. Pal highlighted that a ϕ_g of 0.51-0.52 led to the best result when comparing to the experimental data [32]. In the present study, for the calculation, a ϕ_g of 0.51 is used. Finally, the viscosity of the Pickering emulsions (η) is calculated by applying the following equation:

$$\eta_r = 1 + 2.5\left(\frac{\phi_{agg}}{1-\phi_{agg}}\right) = \eta/\eta_c \quad (4)$$

where η_r is the relative viscosity which is defined as the ratio of emulsion viscosity η to continuous phase viscosity η_c which equals 1.38 mPa s in the present study. In Pal's paper, the emulsion viscosity η was calculated using Eq. (4) for each water volume fraction ϕ.

It is also possible to use other models, commonly applied to conventional emulsions, and to assess the extent to which they can be adapted to Pickering emulsions. This is the subject of the following paragraphs. Concerning the elasticity, Princen model was initially developed for

concentrated foams and, later, adapted to traditional emulsions stabilized with surfactants [28]. The model considers that the droplets are in contact. It is based on rigorous theoretical thermodynamic arguments in two dimensions. However, the extrapolation to 3D systems appears less rigorous in terms of thermodynamic basis. It becomes a semi-empirical model for which two parameters have to be fitted to the experimental results. The elastic modulus is defined as:

$$G' = a\left(\frac{\sigma}{R_{32}}\right)\phi^{\frac{1}{3}}(\phi - \phi_c(P)) \quad (5)$$

where a is a dimensionless adjustable parameter, σ is the oil/water interfacial tension, R_{32} the Sauter radius which is the surface to volume mean droplet radius, while ϕ_c(P) is considered as the critical dispersed-phase volume fraction for which the droplets form an interconnected network. In the present study, the radius R_{32} is fixed to 15 10^{-6} m while the value of σ equals 0.049 N m^{-1}. The latter corresponds to the value of the dodecane/water interfacial tension. This value is chosen because it is admitted that the presence of particles attached to the interface does not substantially modify the value of the interfacial tension [41,42]. Two unknown parameters, a and ϕ_c(P), are to be calculated. The critical dispersed-phase volume fraction ϕ_c(P) is determined graphically. It is linearly extrapolated from the beginning of the G' vs ϕ curve (for the lowest values of ϕ considering that ϕ_c(P) = ϕ (G' = 0)). It is clear that the actual value can be lower than the extrapolated one. However, ϕ_c(P) can be viewed as an effective characteristic structural parameter, i.e. related to experimental data, corresponding to the onset of elastic interactions. In the present case, the critical dispersed-phase volume is ϕ_c(P) = 0.39. Finally, a is used as a fitting parameter so that Eq. (5) best approached the experimental data of Fig. 3. The best fit was obtained here for a = 1.61. It should be noted that this value obtained for Pickering emulsions is close to the value of 1.7 reported by Princen for conventional emulsions [28].

Some approaches address both the dependence of viscosity and elasticity to the volume fraction. For example, empirical mathematical expressions such as power laws are commonly used to fit experimental data of both η and *G' vs* ϕ. The dependencies of the viscosity and elastic modulus to the volume fraction are then expressed as:

$$\eta = b\,\phi^{\mathrm{n}} \tag{6}$$

$$G' = c\,\phi^{\mathrm{m}} \tag{7}$$

where b and c are the pre-exponential factors while n and m are the power exponents. The parameters are obtained from the plot of log η *vs* log ϕ (to obtain b and n) and log *G' vs* log ϕ (to obtain c and m). If the model fits, the linear evolution in log-log plot allows the determination of the parameters from the slope and y-intercept. The values obtained in our case are reported in Table 1. A perfect linear evolution is obtained for the elastic modulus (R^2 = 0.97). Conversely, for the viscosity, the data points for the various dispersed volume fractions do not fall on a single line (R^2 = 0.79). Two linear parts can be extracted: for ϕ ranging between 0.1 and 0.45, and between 0.45 and 0.6. Consequently, the power law does not make it possible to describe the evolution of viscosity with ϕ over the whole range of the dispersed phase volume fraction with a single pair of parameters b and n.

Fig. 3 compares numerical values calculated from the models (lines) and the experiments (points) of viscosities and elastic modulus of the Pickering emulsion as a function of the dispersed volume fraction. The parameters of the models used to fit the experimental data are summarized in Table 1.

Table 1. Parameters of the models used to fit experimental data.

Parameters	**Princen**	**Power law**	**Power law**	**Percolation**	**Percolation**
	G'	$\boldsymbol{\eta}$	***G'***	$\boldsymbol{\eta}$	***G'***

Prefactor	a = 1.61	b = 5.7 10^2	c = 3.2 10^5	$\alpha = 0.69$	$\alpha' = 3.5\ 10^5$
Exponent	-	n = 2.56	m = 15.12	$\beta = 3.52$	$\beta' = 4.63$
ϕ_c	ϕ_c(P) = 0.39	-	-	ϕ_c (η) = 0.76	ϕ_c (G') = 0.39
R^2	-	0.79	0.97	0.98	0.97

When the power law model is applied ("η Power law"), the predicted dispersed volume fraction dependence of the emulsion viscosity is poorly reproduced. For water volume fractions lower than 0.5, the calculated viscosities are larger than the experimental ones. Besides, the model cannot reproduce the steep increase of the viscosity with ϕ at large dispersed volume fractions. This result was expected since a given couple of values of b and n is unable to represent the experimental viscosity over the whole range of dispersed volume fractions. On the opposite, Pal approach ("η Pal") represents the viscosity data fairly well up to a volume fraction of 0.50. However, Pal's model is not able to account for the rapid growth in viscosity and the high values reached when ϕ approaches ϕ_g. For Pickering emulsions, Pal's approach considers that ϕ_g is in the vicinity of 0.52 based on his experimental results for O/W systems [32]. The W/O emulsions data presented here agree with Pal considerations as the best fit encountered for this model was for a fixed $\phi_g = 0.51$, which also explains why there is no calculated viscosity after this value in the figure.

As far as the elastic modulus is concerned, a strong disagreement is observed between Princen's model ("*G'* Princen") and the experimental data. The model is not able to account for the abrupt growth of elastic modulus in the vicinity of $\phi = \phi_c$(P). Similar conclusions were already reported by other authors [30,31,43]. It appears that the power law model ("*G'* Power law") is better suited to describe the experimental data. The calculated and experimental elastic moduli are in good agreement over the whole range of dispersed volume fractions. This is a first indication that the emulsion behaves as a conventional colloidal gel [43].

However, the power law approach is more as a mathematical convenient approach than a physical one since it does not provide any explanation of the occurring phenomena. Therefore, a structural approach mathematically close to the previous one but based on physical principles, even if they are only phenomenological, is preferable. On the basis of these remarks, the percolation approach has recently been used to successfully describe the rheology of highly concentrated emulsions [31]. This approach makes it possible to deal with the viscosity and elasticity of suspensions in the same formal framework and appears to be a good candidate to model the rheology of Pickering emulsions.

The percolation model considers that the elastic modulus of the emulsion becomes non-zero above a critical volume fraction of dispersed phase called the percolation threshold (ϕ_c) [31]. At this volume fraction, the number of droplets in contact is large enough to form a continuous network of interconnected droplets allowing the transport of elastic interactions quantified by *G'* which is related to the number of links between the droplets (Fig. 4a). Consequently, the *G'* modulus becomes greater than 0 just beyond ϕ_c (*G'*). Similarly, the viscosity increases considerably as the volume fraction approaches ϕ_c (η) as the system evolves from a viscoelastic liquid state to a viscoelastic solid state (Fig. 4a). In other words, the percolation threshold (ϕ_c (η)) is the critical volume fraction of dispersed phase for which the zero-shear viscosity (Newtonian plateau) starts to diverge.

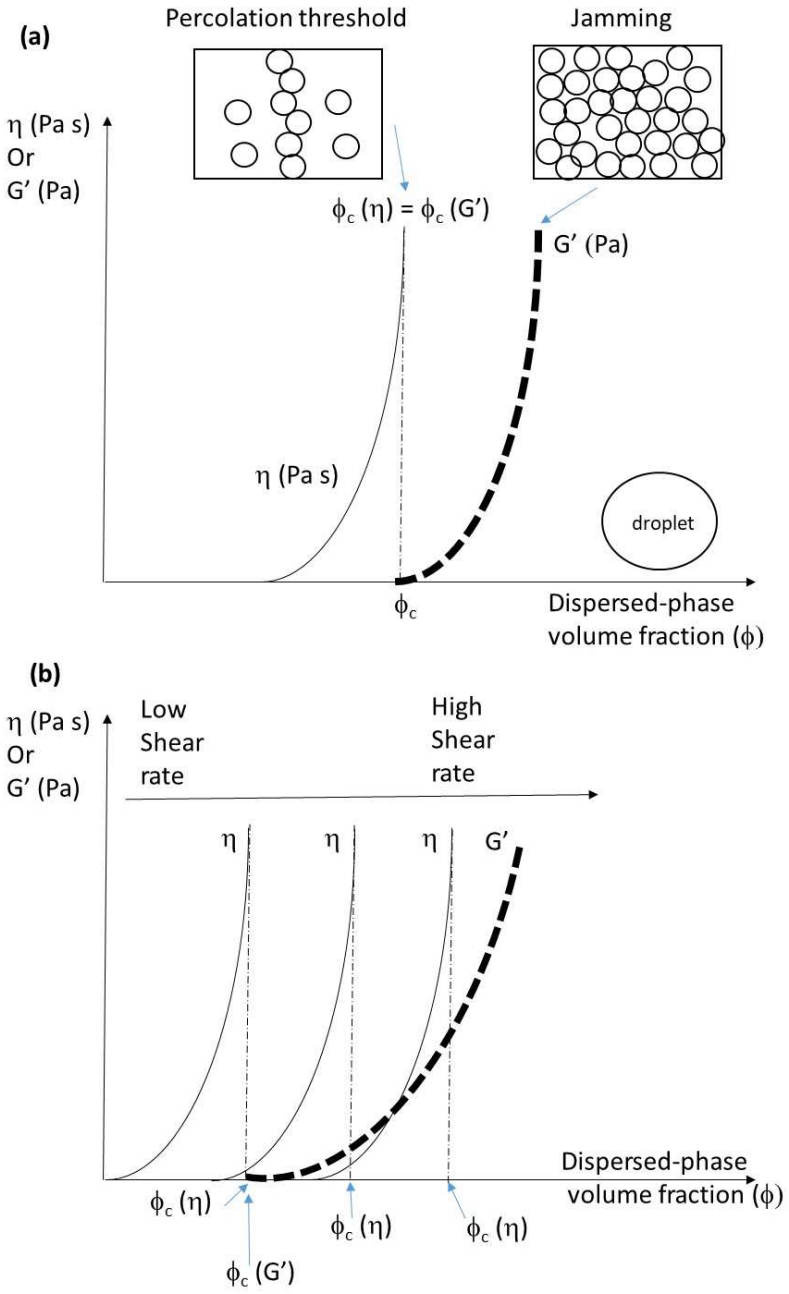

Fig. 4. Percolation model. Schematic representation of (a) the classical evolution of the viscosity at low shear rate (Newtonian plateau) η *vs* ϕ and G' *vs* ϕ when the percolation thresholds ($\phi_c(\eta)$ and $\phi_c(G')$) collapse. (b) Effect of the shear rate on the η *vs* ϕ curves.

The viscosity and the elastic modulus can be expressed as [31]:

$$\eta = \alpha\,(\phi_c(\eta) - \phi)^{-\beta} = \alpha\,\phi_c(\eta)^{\beta}\left(1 - \frac{\phi}{\phi_c(\eta)}\right)^{-\beta} = \eta_c\left(1 - \frac{\phi}{\phi_c(\eta)}\right)^{-\beta} \qquad (8)$$

$$G' = \alpha' (\phi - \phi_c (G'))^{\beta'} = \alpha' \phi_c(G')^{-\beta'} \left(\frac{\phi}{\phi_c(G')} - 1\right)^{\beta'} = G_0' \left(\frac{\phi}{\phi_c(G')} - 1\right)^{\beta'} \quad (9)$$

where α and α' are adjustable parameters, β and β' positive exponents, while $\phi_c(\eta)$ and $\phi_c(G')$ are the percolation thresholds. The aim of the percolation model is to give interpretation and physical information on rheological data. Actually, all the parameters have a physical meaning. The prefactor α is related to the viscosity of the continuous phase (η_c). It appears that $\alpha = \eta_c \phi_c(\eta)^{-\beta}$ (Eq. (8)). Similarly, for the elastic modulus, $\alpha' = G_0' \phi_c(G')^{\beta'}$ (Eq. (9)). The power law exponents, β and β', are critical exponents which are associated to a peculiar phenomenon. In some cases, this power law exponent can be linked to fractal dimensions and to the organization of the dispersion.

This approach based on the percolation theory is well suited to reproduce the steep increase of η and G' for ϕ close to ϕ_c [31]. Several unknown parameters need to be estimated: α, α', $\phi_c(\eta)$, $\phi_c(G')$, β and β'. The percolation threshold $\phi_c(G')$ was determined classically by fitting linearly the first experimental points of G' *vs* ϕ curves, corresponding to low values of ϕ, and by determining the intersection of this line with the x-axis such that $\phi_c(G') = \phi(G' = 0)$ for the elastic modulus. For the viscosity, the percolation threshold $\phi_c(\eta)$ was determined in the zone where the viscosity diverges and tends toward infinity (Fig. 4). The obtained percolation thresholds thus were $\phi_c(\eta) = 0.76$ and $\phi_c(G') = 0.39$. The other parameters were obtained by plotting log η *vs* log ($\phi_c(\eta)$ - ϕ) (to obtain α and β) and log G' *vs* log (ϕ - $\phi_c(G')$) (to obtain α' and β'). This linearization procedure, justified by the values of the linear regression coefficients (R^2 = 0.98 for η and R^2 = 0.97 for G'), allows the determination of the parameters from the slope and y-intercept of the curves. The values are reported in Table 1. It is interesting to note that the percolation thresholds $\phi_c(\eta)$ and $\phi_c(G')$ take different values. $\phi_c(\eta)$ is affected by the shear rate. Actually, the η *vs* ϕ curves shift to larger $\phi_c(\eta)$ when the

shear rate increases (Fig. 4b). This shift is due to the fact that the emulsions are shear-thinning and thixotropic, inducing a decrease of their viscosity by increasing the shear rate. Consequently, under shear, a denser packing of droplets can be reached leading to an increase of $\phi_c(\eta)$ because, in absence of shear, droplets aggregates are rather open while, under shear, droplets aggregates rearrange to a more compact structure. Consequently, $\phi_c(\eta)$ increases with the shear rate. Based on this reasoning, the $\phi_c(\eta)$ coincides with $\phi_c(G')$ only at very low shear rates corresponding to the Newtonian plateau. In the present study, $\phi_c(\eta)$ is different from $\phi_c(G')$ because the viscosity values were recorded at a shear rate of 100 s^{-1}. The viscosity was measured at this high shear rate to ensure a better measurement sensitivity. Consequently, the shear rate is too large to reach $\phi_c(\eta) = \phi_c(G')$. The value which needs to be discussed is $\phi_c(G')$. It is not impacted by the shear rate since it has been determined within the linear viscoelastic domain of the samples. $\phi_c(G')$ is characteristic of the connectivity inside the volume of emulsion, *i.e.* the threshold of percolation and the link between the droplets. On the other hand, $\phi_c(\eta)$ is an effective percolation threshold only used for the fit at a given shear rate.

We checked the validity of the percolation model by comparing calculated and experimental viscosity and elastic modulus as a function of the dispersed volume fraction. The results are shown in Fig. 5. A very good agreement between the percolation model and experimental viscosity data is found. The percolation approach accounts for almost all data points. The ϕ dependence of η is well described even at the largest volume fractions (higher than 0.5). The same trends are observed and the same conclusions can be drawn regarding the elastic modulus. It is important to note that the percolation model is the only one that quantitatively and accurately describes the experimental data over the entire range of dispersed volume fractions, for both viscosity and elastic modulus. This is quite an interesting result since the viscosity and the elastic modulus are significantly affected for medium and

large dispersed volume fractions, respectively. The increase of both the viscosity and the elastic modulus are sharp. The percolation model captures the essence of the physics underlying the dependence of rheological behavior on the volume fraction of the dispersed phase for both viscosity and elasticity and, more particularly, it accounts fairly well for the transition from intermediate to concentrated dispersed volume fractions where η and G' increase abruptly. Besides, it has been shown that a first-order Taylor expansion of the percolation model (Eq. (9)) leads to an expression similar to that of Princen and Kiss model [31]. In the same spirit, a simple rearrangement by factorization of ϕ_c (η) in Eq. (8) leads to an expression similar to Krieger-Dougherty and Quemada [44-47] (right part of Eq. (8)). Therefore, due to its integrative nature, the percolation model alone will be used to analyze the results in the rest of the article.

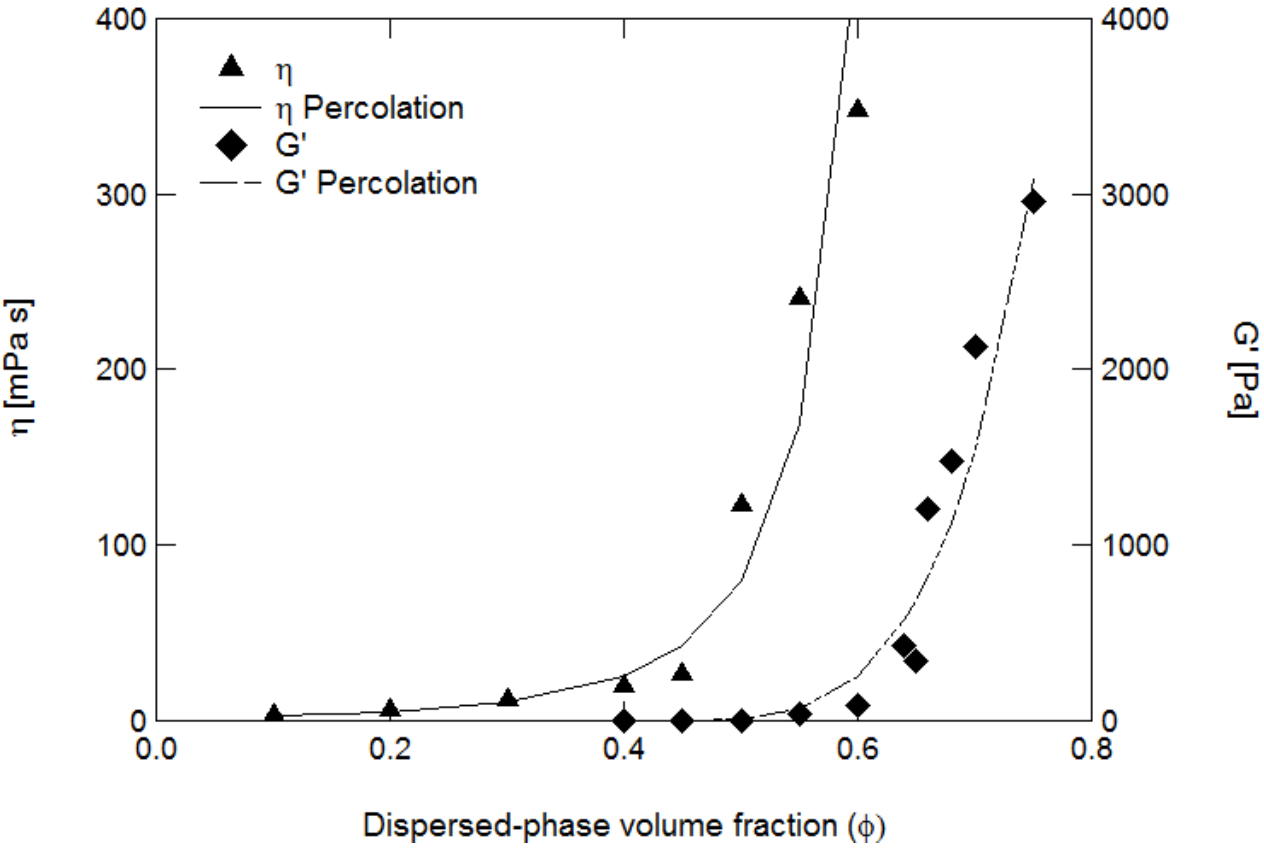

Fig. 5. Comparison of experimental and percolation-model data of viscosity and elastic modulus as a function of the volume fraction of the dispersed phase. The percolation model was fitted to experimental data using Eqs. (8-9).

The values obtained with the percolation approach for the viscosity can be discussed more particularly. The best agreement with the experimental values of viscosity is obtained with $\phi_c(\eta)$ = 0.76, $\beta = 3.52$ and α = 0.69 (Table 1). The exponent β may appear quite large compared to the coefficient of Quemada's equation $\beta = 2$. This high exponent value, together with the low percolation threshold, is probably indicative of the existence of more complex interactions in Pickering emulsions than in conventional emulsions as it will be shown below (see part 3.2.). Furthermore, the viscosity of the continuous phase η_c can be determined by using $\eta_c = \alpha\, \phi_c(\eta)^{\beta}$ (Eq. (8)), leading the value η_c = 1.812 mPa s. This viscosity is supposed to be the viscosity of the continuous phase in the absence of droplets. This value appears larger than that of the pure dodecane oil (1.38 mPa s) indicating that silica particles are present in the continuous phase. From η_c, the particle concentration in the continuous phase can be estimated (see Supporting information Calculation S1 for details of calculation). A viscosity of 1.812 mPa s corresponds to a silica mass fraction of 2.77 wt.% in the continuous phase. The emulsion should therefore be considered as a dispersion of water droplets, covered with silica particles, immersed in a suspension of silica in oil at an average concentration of 2.77 wt.%. This silica mass fraction appears larger than the theoretical silica contents remaining in the continuous phase in the presence of a silica monolayer attached to the droplets ($\varepsilon_{continuous,monolayer}$, Table S1 of the Supporting Information). In this reasoning, it is emphasized that, in the present Pickering emulsion, the silica particles seem to be mostly dispersed in the continuous phase rather than at the interfaces of the droplets. Furthermore, this suggests that the number of particle layers at the droplet interface is relatively small and

even less than one. However, it is important to keep in mind that (i) the calculation of η_c was only an indicative calculation to check the consistency of the fitting parameter and (ii) the estimation of an amount of silica particles in the continuous phase was just a preliminary step which seems to indicate that some silica particles might be present in the continuous phase. All these aspects will be confirmed in the next section.

3.2. Comparison of the rheological behavior of Pickering and classical emulsions

In this section, we compare the dependence of the elastic modulus to the dispersed volume fraction for the W/O Pickering emulsion stabilized by silica particles with those of classical emulsions stabilized with surfactants. The difference between the rheological behavior of the two emulsion types is used to discuss the repartition of the particles in the emulsions, *i.e.* at the W/O interfaces and/or in the continuous phase.

Several systems of emulsions stabilized with molecular surfactants are investigated. First, water-in-dodecane emulsions are considered. These reverse emulsions are stabilized by mixtures of non-ionic surfactants to obtain different formulations, with HLB values of 5.6, 7.7, and 10 (respectively named « W/Dodecane HLB 5.6 », « W/Dodecane HLB 7.7 », and « W/Dodecane HLB 10 »). The data were obtained in our laboratory from the work of Paruta-Tuarez et al. [30]. The size of the water droplets ranges from around 3 to 16 µm depending on the HLB value and the dispersed phase volume fraction. It is important to mention that the oil used is the same for Pickering and classical emulsions, the only difference being the presence of particles (Pickering emulsion) or surfactants (classical emulsions). However, the droplet size is larger with Pickering emulsion (20-30 µm). This behavior was already reported in several instances [5,7,27]. In addition, oil-in-water direct emulsions are also investigated. On the one hand, concentrated decane-in-water emulsions were obtained in presence of ABA block copolymer composed of polyethylene oxide – polypropylene oxide – polyethylene

oxide. The experimental results were previously reported by Pons et al. [25]. Droplets of decane with diameters of 2.9-3.2 µm are observed. On the other hand, kerosene-in-water emulsions prepared with Triton X 100 as surfactant are also considered thanks to the experimental data previously obtained by Pal [26]. The average size of kerosene droplets is about 2.8 µm. The two O/W emulsions are denoted by « Decane/Water » for decane-in-water emulsions and « Kerosene/Water » for kerosene-in-water emulsions. All these systems (O/W and W/O classical emulsions) are chosen to scan a large range of rheological behavior.

In Fig. 6, the reported elastic modulus for emulsions stabilized by surfactants and Pickering emulsion are plotted against the dispersed phase volume fraction. Note that the percolation thresholds ϕ_c (G') of classical emulsions were determined in a similar manner as for Pickering emulsion to ensure a consistent comparison, the resulting values being reported in Table 2. The Fig. 6 shows that the values and evolution of the elastic modulus depend strongly on the nature of the stabilizer, *i.e.* surfactants or particles. Therefore, the data can be divided into two categories depending on the presence or absence of particles. For emulsions stabilized by surfactants, *i.e.* in the absence of particles, each curve shows similar trends characterized by a smooth and gradual increase in *G'*. Conversely, for the particle-stabilized emulsion, the experimental results show a steeper increase in *G'* for a much lower value of the volume fraction of the dispersed phase and *G'* reaches larger values with particles than with surfactants. The presence of particles therefore enhances the elasticity of the emulsion. It is now well established that the presence of particles at the W/O interface improves more efficiently the interface elasticity than surfactants [3,4,11] and contributes to the increase in the elastic modulus of the Pickering emulsion. In addition, as mentioned above, the sudden increase of *G'* occurs for lower ϕ in the presence of particles than for surfactants. Correlatively, while the percolation threshold ϕ_c (G') is equal to 0.84-0.85 for Water/Dodecane classical emulsions, 0.64 for Kerosene/Water and 0.76 for Decane/Water

systems, it reaches 0.39 for the Pickering emulsion. This low percolation threshold value, in the presence of particles, was also highlighted by Xiao et al. [22]. They reported a shift of the rheological properties from viscous dominant behavior at $\phi = 0.3$ to elastic dominant behavior at $\phi = 0.5$ and $\phi = 0.7$ for O/W (soybean oil) emulsions in the presence of 0.5 wt.% of kafirin protein nanoparticles. At volume fractions of 0.5 and 0.7, a gel-like structure was highlighted. Bearing in mind that the random close packing fraction of perfect monodisperse rigid spheres corresponds to $\phi = 0.64$, it is important to note that the percolation threshold exceeds this value for classical emulsions while it becomes significantly lower for Pickering emulsions.

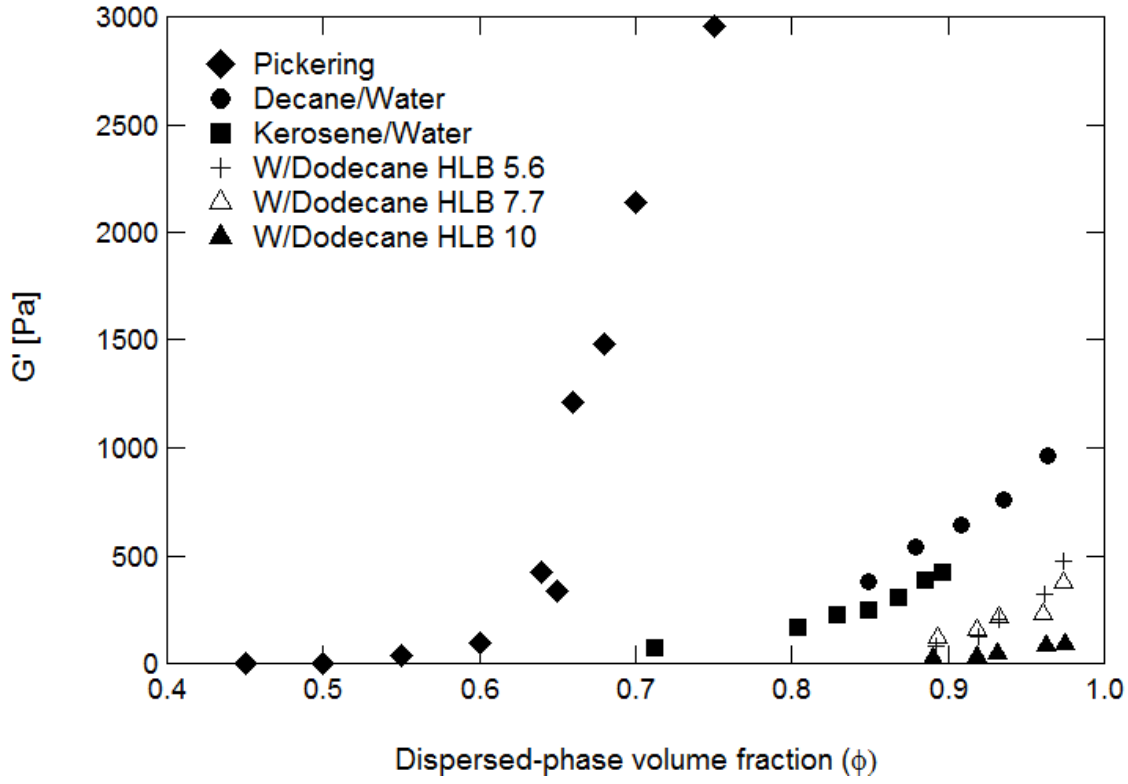

Fig. 6. Comparison of the elastic modulus of a Pickering emulsion ("Pickering") with those of surfactant-stabilized O/W (decane/water and kerosene/water) and W/O (water/dodecane) emulsions as a function of the dispersed-phase volume fraction (ϕ).

The substantial difference between the data with Pickering and classical emulsions can be explained by the presence of the particles. Droplet percolation occurs at lower dispersed phase values in the presence of particles than with surfactants. In the Pickering emulsion, the particles form contact chains inducing a connection between the droplets leading to a network of droplets/particles. As a consequence, elastic interactions develop through the sample for lower fractions of dispersed phase than in conventional emulsions due to the droplet/particle contact network. Two main kinds of particles organization could explain this phenomenon. On the one hand, the link between the droplets could be ensured through the network of particles in the continuous phase (Fig. 7a). The particles in the continuous phase, filling the gap between the droplets, can form bridges linking them together. On the other hand, the presence of particles adsorbed onto droplet surface could be sufficient to increase their apparent volume fraction leading to an effective volume fraction ϕ_{eff} larger than ϕ (Fig. 7b). Consequently, the percolation process would occur at lower values of ϕ due to the thickness of the adsorbed layer.

The distinction between both mechanisms can be analyzed through the evaluation of the number of adsorbed particles on the droplets which produces the effective volume fraction ϕ_{eff} needed to reach the percolation. The effective volume fraction of the droplets in the case of multi-layered oil/water interfaces is given by:

$$\phi_{eff} = \phi \left(1 + \frac{Nl\, d_p}{R_d}\right)^3 \quad (10)$$

where *Nl* is the number of layers of particles attached to the droplets (Fig. 7d).

For a monolayer of nanoparticles at the interface (*Nl* = 1), the calculated values of ϕ_{eff} are very close to those of ϕ (Table S2 and Fig. S2 of the Supporting Information). The difference ϕ_{eff} - ϕ is around 0.002 which is negligible. This indicates that the contribution of the silica

monolayer is not sufficient to explain the difference in rheological behavior observed between emulsions stabilized by silica particles and those stabilized by surfactants.

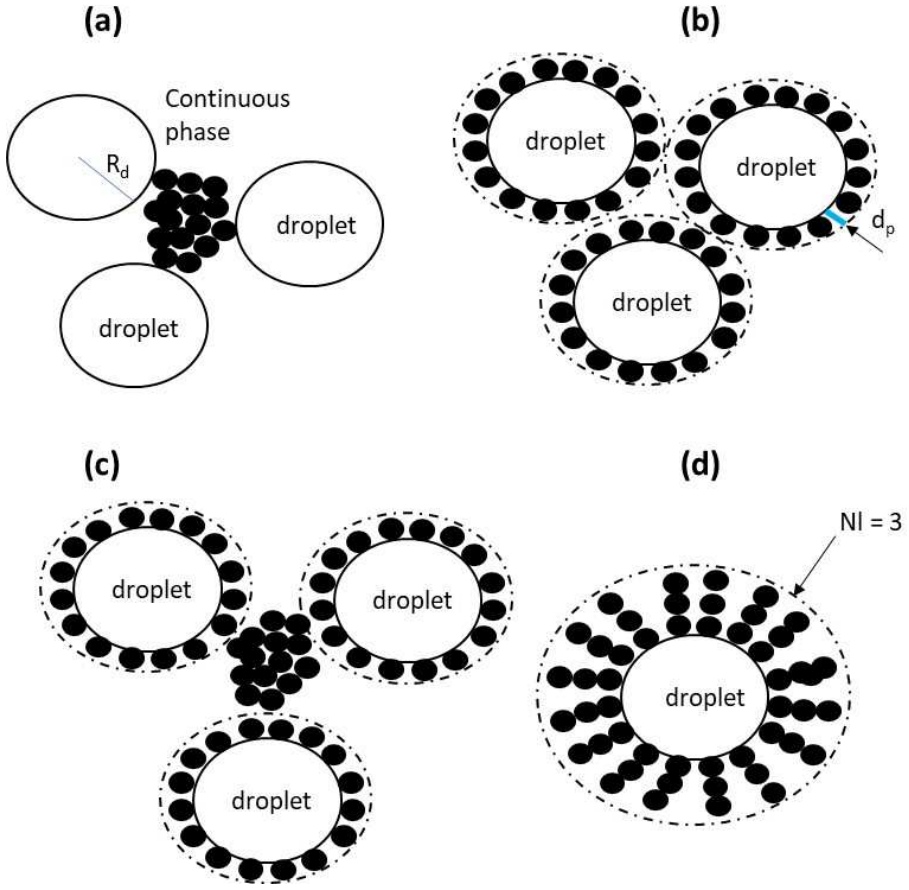

Fig. 7. Schematic representation of the possible modes of contact between the droplets for Pickering emulsions. (a) Particles network in the continuous phase. The particles are located in the interstitial fluid and form bridges between the droplets. (b) Particles adsorbed onto the droplets. (c) Coexistence of the 2 modes. (d) Droplet in the presence of multiple layers of solid particles (Nl = 3 layers) at the oil/water interface for the estimation of the effective volume fraction ϕ_{eff}.

However, a substantial increase in the number of particle layers adsorbed on the droplets could produce a significant increase of ϕ_{eff}. The results of Fig. 6 can be replotted as a function of the effective volume fraction ϕ_{eff} rather than the volume fraction of bare droplets. Curves with surfactants are not affected due to the extreme thinness of the surfactant layer, it can be

assumed that $\phi_{eff} = \phi$ in that case. Therefore, the calculation was only conducted with Pickering emulsion. The idea was to rescale the x-axis (ϕ_{eff}) by modifying the number of layers of particles attached to the droplets to make the Pickering curve coincide with those of the surfactants, the only adjustable parameter being *Nl*. Fig. S2 of the Supporting Information compares the rescaled (dotted line) and experimental elastic modulus against the effective volume fraction. Table 2 summarizes the number of particles layers required to rescale the results obtained for Pickering emulsions to those obtained for conventional emulsions. This rescaling procedure applied to O/W emulsions (Decane/Water and Kerosene/water emulsions) stabilized by surfactants leads to *Nl* = 93-95 layers. This means that a layer of particles 1500 nm in thickness would be required to observe a dependence of the elastic modulus of Pickering emulsions with the dispersed phase volume fraction approximately equivalent to that of conventional emulsions. In the same way, the rescaling procedure applied to the water-in-dodecane emulsions stabilized by surfactants gives *Nl* = 137 layers. This number of layers represents a particle layer thickness of 2200 nm at the interface.

Table 2. Comparison of percolation threshold ϕ_c (G') and maximum elastic modulus G'_{max} for Pickering and surfactants-stabilized emulsions (Decane/Water, Kerosene/Water, Water/Dodecane HLB 5.6, HLB 7.7, HLB 10). Number of particles layers needed to rescale the Pickering results to the classical emulsions stabilized by surfactants from Fig. 6 and Fig. S2 (*Nl* rescaling ϕ_{eff}) and from the difference of ϕ_c (G') (*Nl*$_c$ rescaling $\phi_{c,eff}$).

Type of emulsion	Pickering	Water/ Dodecane HLB 5.6	Water/ Dodecane HLB 7.7	Water/ Dodecane HLB 10	Decane/ Water	Kerosene/ Water
Parameters						
ϕ_c (G')	0.39	0.85	0.84	0.85	0.76	0.64
G'_{max} (Pa)	2954	474	369	89	960	420

Number of layers	-	137	137	137	95	93
Nl rescaling ϕ_{eff}						
Number of layers	-	275	275	275	236	170
Nl_c rescaling $\phi_{c,eff}$						

In a more quantitative way, it appears relevant to estimate the number of particle layers Nl_c attached to the droplets in order to reach the percolation threshold ϕ_c (G') of the classical emulsions stabilized with surfactants with those of the Pickering emulsion $\phi_{c,eff}$ (see Supporting Information calculation S2 for details of calculation). The percolation thresholds ϕ_c (G') of conventional emulsions stabilized with surfactants have been estimated to be 0.64, 0.76 and 0.85 for Kerosene/water, Decane/Water and Water/Dodecane emulsions, respectively (Table 2). The respective numbers of particle layers (Nl_c) covering the droplets required to make the percolation threshold of Pickering emulsions $\phi_{c,eff}$ coincide with those of conventional emulsions ϕ_c (G') are 170, 236 and 275 layers. Thus, both assessments give the same order of magnitude of the number of particles layers needed to reach the percolation threshold. However, it is not realistic that such large amounts of particles can be adsorbed at the W/O interfaces since, according to the number of particles introduced in the emulsion, the theoretical number of possible layers is equal to 2.37 if all the particles are adsorbed (see Eq. (1) and Table S1 of the Supporting Information). This emphasizes that droplets binding cannot be attributed solely to the layers of particles adsorbed at the interfaces and that the particles suspended in the continuous phase make a major contribution to droplets connectivity (Fig. 7a). As a result, these particles contribute significantly to the elastic modulus and viscosity values of Pickering emulsions, probably through the formation of a viscoelastic 3-dimensional network of interconnected particles and droplets. This kind of 3D network has already been reported with silica for O/W emulsions and with clays

[14,15,18,20,21,48]. However, one should be aware that both contributions (interfacial layer and particle network in the continuous phase) can significantly affect the rheological behavior of Pickering emulsions (Fig. 7c). Numerous situations could occur depending on the particle's nature and oil types, i.e. on the particle/oil/water contact angle [11]. Two extreme situations can be encountered. First, all the particles may be strongly anchored at the liquid/liquid interface (Fig. 7b). This kind of configuration is largely reported in the literature [14-17]. On the opposite, the particles may not adsorb at all or only weakly on the droplets but are present in the continuous phase (Fig. 7a) [49,50]. However, in some cases, both configurations take place simultaneously (Fig. 7c). The particles are not only located at the interface but also aggregate in the continuous phase [48]. In the present study, a significant amount of the particles are located in the continuous phase. This is not surprising based on the value of the silica/water/dodecane contact angle which is around 114° [33].

To assess this hypothesis, the silica amount in the continuous oil phase can be evaluated. When taking into account the amount of silica necessary to form a monolayer at the droplets interfaces, the remaining fraction of silica in the continuous phase $\varepsilon_{continuous,monolayer}$ becomes around 1.12 and 1.84 wt.% (Table S1 of the Supporting Information). These values appear sufficient to ensure the formation of the 3D network between the droplets. However, it remains difficult to directly compare them with those reported in the literature with clays and silica for Pickering emulsions since they greatly depend on the ionic strength, pH, nature of particles and dispersed volume fraction [14-16]. Under certain conditions, gels can be obtained with 1 wt.% of clay while 10 wt.% are required under different conditions with the same material. In the same way, large deviations in the percolation threshold can be expected depending on the silica nature and surrounding environment (oil, water, salt nature and concentrations).

To complete the above analysis, it is interesting to note that the maximum *G'* value is reported with the emulsion containing a dispersed phase fraction of 0.75 in the presence of 1 wt.% of silica. Separate experiments reveal that an emulsion prepared with an aqueous dispersed phase fraction of 0.66 and a silica fraction of 2 wt.% exhibits a similar rheological behavior (Fig. 8). In particular, they show comparable values of plateau modulus G' and critical strain. At these volume fractions considered here, the random close packing fraction is already reached and the droplets are in close contact regardless of the concentration of silica particles. Consequently, an amount of particles of 1.84 wt.% (or maybe less) is sufficient to strengthen the network of particles between the droplets (Table S1 of the Supporting Information). Reducing the droplet volume fraction to 0.66, leads to a larger space in the continuous phase between the droplets. Consequently, a larger particle content in the continuous phase becomes necessary to reinforce the network and reach the same value of G'. Under the conditions of this study, considering that a monolayer of particles is adsorbed on the droplet surface, a particle content of 3.34% by weight in the continuous phase is available to contribute to the reinforcement of the network (Table S1 of the Supporting Information). These results suggest that the rheological behavior of these emulsions can be adjusted, and therefore controlled, through two different paths: obviously, through the volume fraction of the dispersed phase but also by modulating the quantity of particles dispersed in the continuous phase. This latter aspect has been already described [49,50]. The authors demonstrated that the rheological properties of Pickering emulsions can readily be tuned by the excess particles added in the continuous phase. This opportunity provides a very practical formulation tool for product and process design and it is clear that the organization of particles at the interface and in the continuous phase must be considered in any modelling attempt which will be the subject of future work.

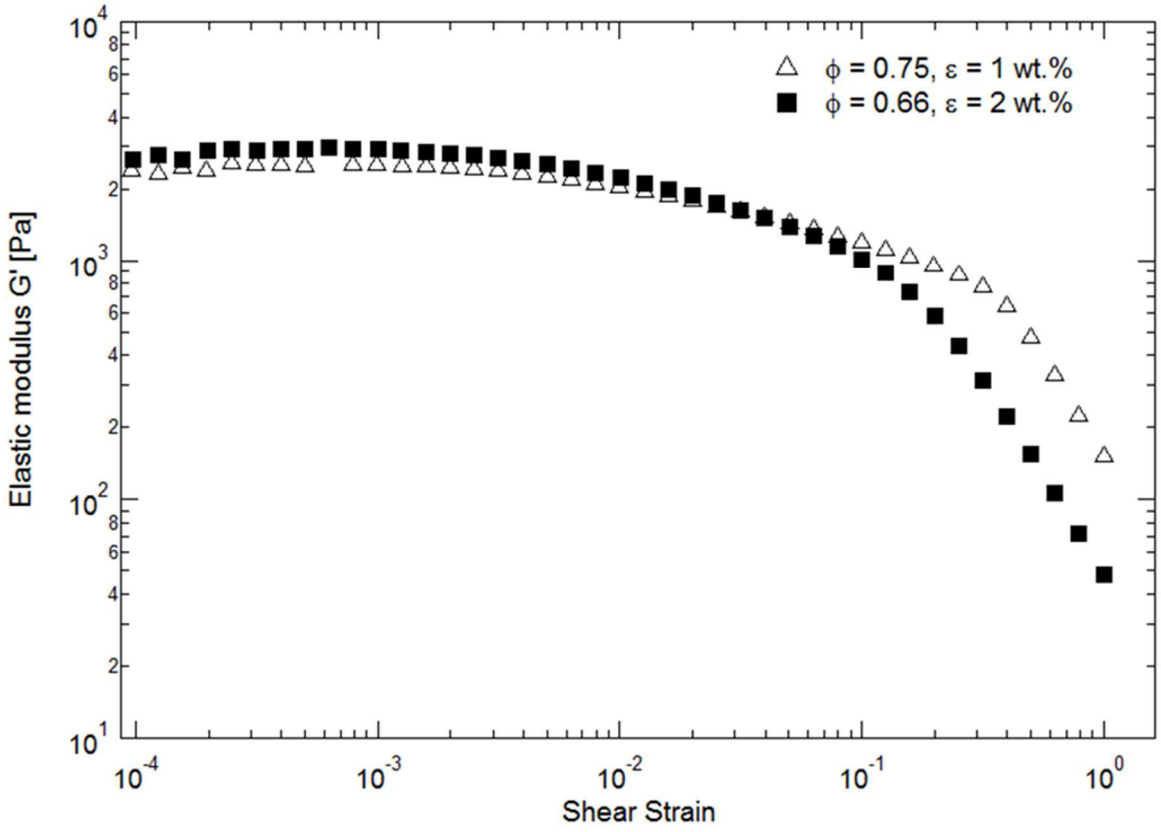

Fig. 8. Comparison of the rheological properties of emulsions containing a disperse phase fraction of 0.75 in the presence of 1% by weight of silica (ϕ = 0.75, ε = 1%) with that prepared at 0.66 of disperse phase fraction and 2% by weight of silica (ϕ = 0.66, ε = 2%). Elastic modulus of reverse Pickering emulsions against shear strain for the two emulsions. The NaCl concentration (λ) is fixed to 1 wt.%.

4. Conclusion

The rheological behavior of water-in-dodecane emulsions stabilized with hydrophobic silica nanoparticles was investigated. Shear viscosity and elastic modulus of emulsions were characterized at dispersed phase volume fractions ϕ varying from 0.1 to 0.75. In flow regime, a sharp increase in viscosity for ϕ greater than 0.3 and a divergence ($\eta \to \infty$) at a critical volume fraction of the order of 0.6 was obtained. Measurements in oscillatory regime indicated that emulsions acquired elasticity at a second critical volume fraction of dispersed

phase of about 0.4 beyond which the elastic modulus increased strongly. Several rheological models were used to fit experimental data. The percolation model was the only one that could accurately reproduce the experimental data, both in steady state (viscosity) and oscillatory regime (elastic modulus) in the whole range of ϕ, hence, providing a unified description of the rheological behavior of the Pickering emulsions.

The comparison of the evolution of the elastic modulus of the Pickering emulsion with those of emulsions stabilized with surfactants showed a significant shift of the curves to higher percolation thresholds. This substantial difference was explained by the presence of the particles at the oil/water interface and in the continuous phase. They allowed an interconnection of the droplets for a lower dispersed phase content than in conventional emulsions leading to the formation of a continuous network which insured elasticity transport corresponding to $G' \neq 0$. The number of layers of particles attached to the droplets required to reach the effective volume fraction corresponding to the percolation threshold was estimated to lie between 93 and 275 layers. The link between the droplets cannot be only attributed to interfacial layers of particles. These results suggested the existence of a mixed 3D-network of interconnected particles and droplets that provided a major contribution to the droplet connections. In terms of elasticity transport, an equivalent viscoelastic 3D-network was obtained preparing emulsions at $\phi = 0.66$ and 2 wt.% of silica or at $\phi = 0.75$ with 1 wt.% of particles. Conversely, when the majority of the particles are adsorbed on the droplets rather than in the continuous phase, the percolation threshold is shifted towards values of larger volume fractions similar to that of surfactant stabilized emulsions.

The results presented provide then a useful methodology to study the distribution of particles in Pickering emulsions through the evolution of their rheological characteristics analyzed using a percolation-type approach. This methodology needs to be compared to the other techniques developed to evaluate the distribution of particles in emulsions (Table 3).

Microscopic techniques including confocal laser scanning microscopy and transmission electron cryomicroscopy (CryoTEM), remain the most used approaches [51-59]. They allow a direct visualization of the repartition of the particles inside the emulsions but present some limitations such as the long duration experiment, possible artifacts due to the sample preparation, or a too local measurement. Consequently, they could not be fully representative of the whole volume of the emulsions. Some gravimetric techniques have been also developed to estimate the amount of particles inside the continuous phase after natural or forced (centrifugation) separation of the emulsions [21,60]. These methods give a quantitative estimation of the amount of particles in the continuous phase but do not give access to their organization. Some errors can occur during the separation process due to a partial desorption of the particles from the oil/water interface. While all these techniques are very efficient, they need to be coupled to another one to obtain a complete picture of the distribution of the particles in the whole volume of the emulsions. The rheological methodology developed in our work can be considered as a complementary approach to study the emulsion characteristics in terms of particle distribution within the volume and not destructive approach.

Future work will address the validation of the rheological methodology with other Pickering systems. For instance, oil-in-water Pickering emulsions can be tested with particles with different surface wettability and/or size. In the same way, the use of hard and soft particles as well as mineral and organic particles will be a good way to test the validity and the limitations of the rheological approach.

Table 3. Summary and comparison of the existent techniques to evaluate the distribution of particles in emulsions. The techniques can be classified on the basis of two parameters: qualitative *vs* quantitative and local *vs* global (all the volume of the sample).

Technique	Quantitative	Qualitative	Global	Local	References
Confocal laser scanning microscopy	-	+	-	+	[51-55]
Transmission electron cryomicroscopy	-	+	-	+	[56-59]
Gravimetry	+	-	+	-	[21,60]
Atomic force microscopy	-	+	-	+	[56,61]
Neutron reflectometry	+	-	-	+	[62,63]
Raman spectroscopy	+	-	+	-	[64]
Gel trapping technique	-	+	-	+	[65]

References

[1] W. Ramsden, Separation of solids in the surface-layers of solutions and "suspensions" (Observations on Surface-Membranes, Bubbles, Emulsions, and Mechanical Coagulation). -- Preliminary Account, Proc. R. Soc. Lond. 72 (1903) 156.

[2] S. U. Pickering, CXCVI.—Emulsions, J. Chem. Soc. Trans. 91 (1907) 2001.

[3] V. Schmitt, M. Destribats, R. Backov, Colloidal particles as liquid dispersion stabilizer: Pickering emulsions and materials thereof, C. R. Physique 15 (2014) 761-774.

[4] Y. Chevalier, M.A. Bolzinger, Emulsions stabilized with solid nanoparticles: Pickering emulsions, Colloids Surf. A 439 (2013) 23-34.

[5] J. Wu, G-H Ma, Recent studies of Pickering emulsions: particles make the difference, Small 12 (2016) 4633–4648.

[6] Y. Yang, Z. Fang, X. Chen, W. Zhang, Y. Xie, Y. Chen, Z. Liu, W. Yuan, An overview of Pickering emulsions: Solid-particle materials, classification, morphology, and applications, Front. Pharmacol. 8 (2017) 287.

[7] C. Albert, M. Beladjine, N. Tsapis, E. Fattal, F. Agnely, Huang, Pickering emulsions: Preparation processes, key parameters governing their properties and potential for pharmaceutical applications, J. Control. Release 309 (2019) 302-332.

[8] S. Lam, K.P. Velikov, O.D. Velev, Pickering stabilization of foams and emulsions with particles of biological origin, Curr. Opin. Colloid Interface Sci. 19 (2014) 490-500.

[9] K.Y. Yoon, H.A. Son, S.K. Choi, J.W. Kim, W. M. Sung, H. T. Kim, Core flooding of complex nanoscale colloidal dispersions for enhanced oil recovery by in situ formation of stable oil-in-water Pickering emulsions, Energy Fuels 30 (2016) 2628−2635.

[10] H. Zhou, X.L. Cao, L.L. Guo, Z.Y. Guo, M. Liu, L. Zhang, S. Zhao, Studies on the interfacial dilational rheology of films containing heavy oil fractions as related to emulsifying properties, Colloids Surf. A 541 (2018) 117–127.

[11] M. Destribats, S. Gineste, E. Laurichesse, H. Tanner, F. Leal-Calderon, V. Héroguez, V. Schmitt, Pickering emulsions: What are the main parameters determining the emulsion type and interfacial properties? Langmuir 30 (2014) 9313–9326.

[12] F. Leal-Calderon, V. Schmitt, Solid-stabilized emulsions, Curr. Opin. Colloid Interface Sci. 13 (2008) 217–227.

[13] T.S. Horozov, B.P. Binks, Particle-stabilized emulsions: A bilayer or a bridging monolayer? Angew. Chem. Int. Ed. 45 (2006) 773–776.

[14] D. Kpogbemabou, G. Lecomte-Nana, A. Aimable, M. Bienia, V. Niknam, C. Carrion, Oil-in-water Pickering emulsions stabilized by phyllosilicates at high solid content, Colloids Surf. A 63 (2014) 85-92.

[15] T.S. Horozov, B.P. Binks, T. Gottschalk-Gaudig, Effect of electrolyte in silicone oil-in-water emulsions stabilized by fumed silica particles, Phys. Chem. Chem. Phys. 9 (2007) 6398–6404.

[16] T. Young Jeon, J. Sook Hong, Stabilization of O/W emulsion with hydrophilic/hydrophobic clay particles, Colloid Polym. Sci. 292 (2014) 2939-2947.

[17] D.J. French, P. Taylor, J. Fowler, P.S. Clegg, Making and breaking bridges in a Pickering emulsion, J. Colloid Interface Sci. 441 (2015) 30–38.

[18] M.V. Mironova, S.O. Ilyin, Effect of silica and clay minerals on rheology of heavy crude oil emulsions, Fuel 232 (2018) 290-298.

[19] M. Kaganyuk, A. Mohraz, Non-monotonic dependence of Pickering emulsion gel rheology on particle volume fraction, Soft Matter 13 (2017) 2513–2522.

[20] W.J. Ganley, J.S. van Duijneveld, Controlling the rheology of montmorillonite stabilized oil-in-water emulsions, Langmuir 33 (2017) 1679−1686.

[21] T. Fuma, M. Kawaguchi, Rheological responses of Pickering emulsions prepared using colloidal hydrophilic silica particles in the presence of NaCl, Colloids Surf. A 465 (2015) 168-174.

[22] J. Xiao, X. Wang, A.J. Perez Gonzalez, Q. Huang, Kafirin nanoparticles-stabilized Pikering emulsions: Microstructure and rheological behavior, Food Hydrocoll. 54 (2016) 30-39.

[23] S.R. Derkach, Rheology of emulsions, Adv. Colloid Interface Sci. 151 (2009) 1-23.

[24] J. Chen, R. Vogel, S. Werner, G. Heinrich, D. Clausse, V. Dutschk, Influence of the particle on the rheological behavior of Pickering emulsions, Colloids Surf. A 382 (2011) 238-245.

[25] R. Pons, C. Solans, T.F. Tadros, Rheological behavior of highly concentrated oil-in-water (o/w) emulsions, Langmuir 11 (1995) 1966-1971.

[26] R. Pal, Yield stress and viscoelastic properties of high internal phase ratio emulsions, Colloid Polym. Sci. 277 (1999) 583-588.

[27] U. Bains, R. Pal, In-situ continuous monitoring of the viscosity of surfactant-stabilized and nanoparticles-stabilized Pickering emulsions, Appl. Sci. 9 (2019) 4044-4058.

[28] H.M. Princen, A.D. Kiss, Rheology of foams and highly concentrated emulsions: III. Static shear modulus, J. Colloid Interface Sci. 112 (1986) 427–437.

[29] R. Pal, Influence of interfacial rheology on the viscosity of concentrated emulsions, J. Colloid Interface Sci. 356 (2011) 118-122.

[30] E. Paruta-Tuarez, P. Marchal, V. Sadtler, L. Choplin, Analysis of the Princen and Kiss equation to model the storage modulus of highly concentrated emulsions, Ind. Eng. Chem. Res. 50 (2011) 10359-10365.

[31] E. Paruta-Tuarez, P. Marchal, Association of percolation theory with Princen's approach to model the storage modulus of highly concentrated emulsions, Ind. Eng. Chem. Res. 52 (2013) 11787–11791.

[32] R.A. Pal, A simple model for the viscosity of Pickering emulsions, Fluids 3 (2018) 2-15.

[33] S. Simon, S. Theiler, A. Knudsen, G. Øye, J. Sjöblom, Rheological properties of particle-stabilized emulsions, J. Dispers. Sci. Technol. 31 (2010) 632–640.

[34] D. Pradilla, W. Vargas, O. Alvarez, The application of a multi-scale approach to the manufacture of concentrated and highly concentrated emulsions, Chem. Eng. Res. Des. 95 (2015) 162–172.

[35] S. Arditty, V. Schmitt, J. Giermanska-Kahn, F. Leal-Calderon, Materials based on solid-stabilized emulsions, J. Colloid Interface Sci. 275 (2004) 659–664.

[36] K.A. Ramisetty, A.B. Pandit, P.R. Gogate, Ultrasound assisted preparation of emulsion of coconut oil in water: Understanding the effect of operating parameters and comparison of reactor designs, Chem. Eng. Process. 88 (2015) 70-77.

[37] N. Mollakhalili Meybodi, M.A. Mohammadifar, KH. Abdolmaleki, Effect of dispersed phase volume fraction on physical stability of oil-in-water emulsion in the presence of gum tragacanth, J. Food Qual. Hazards Control 1 (2014) 102-107

[38] S.G. Gaikwad, A.B. Pandit, Ultrasound emulsification: Effect of ultrasonic and physicochemical properties on dispersed phase volume and droplet size, Ultrason. Sonochem. 15 (2008) 554-563.

[39] O.A. Alvarez, L. Choplin, V. Sadtler, P. Marchal, M.J. Stébé, J. Mougel, C. Baravian, Influence of semibatch emulsification process conditions on the physical characteristics of highly concentrated water-in-oil emulsions, Ind. Eng. Chem. Res. 49 (2010) 6042–6046.

[40] E. Paruta-Tuarez, V. Sadtler, P. Marchal, L. Choplin, J.L. Salager, Making use of the formulation-composition map to prepare highly concentrated emulsions with particular rheological properties. Ind. Eng. Chem. Res. 50 (2011) 2380–2387.

[41] A. Drelich, F. Gomez, D. Clausse, I. Pezron, Evolution of water-in-oil emulsions stabilized with solid particles: Influence of added emulsifier, Colloids Surf., A 365 (2010) 171−177.

[42] A.P. Kotula, S.L. Anna, Probing timescales for colloidal particle adsorption using slug bubbles in rectangular microchannels, Soft Matter 8 (2012) 10759−10772.

[43] V. Trappe, V. Prasad, L. Cipelletti, P. N. Segre, D.A. Weitz, Jamming phase diagram for attractive particles, Nature 411 (2001) 772-775.

[44] M. Mooney, The viscosity of a concentrated suspension of spherical particles, J. Colloid Sci. 6 (1951) 162–170.

[45] I. M. Krieger, T. J. Dougherty, A mechanism for non-Newtonian flow in suspensions of rigid spheres, Trans. Soc. Rheol. 3 (1959), 137–152.

[46] D. Quemada, Rheology of concentrated disperse systems and minimum energy dissipation principle, Rheol. Acta 16 (1977) 82–94.

[47] R. Pal, E. Rhodes, Viscosity/concentration relationships for emulsions, J. Rheol. 33 (1989) 1021-1045.

[48] M. Dinkgreve, K.P. Velikov, D. Bonn, Stability of laponite®-stabilized high internal phase Pickering emulsions under shear, Phys. Chem. Chem. Phys. 18 (2016) 22973-22977.

[49] E. Vignati, R. Piazza, T.P. Lockhart, Pickering emulsions: interfacial tension, colloidal layer morphology, and trapped-particle motion, Langmuir 19 (2003) 6650-6656.

[50] B.R. Midmore, Preparation of a novel silica-stabilized oil/water emulsion, Colloids Surf. A 132 (1998) 257-265.

[51] A. Schroder, M. Laguerre, J. Sprakel, K. Schroen, C.C. Berten-Carabin, Pickering particles as interfacial reservoirs of antioxidants, J. Colloid Interface Sci. 575 (2020) 489-498.

[52] F. Sabri, W. Raphael, K. Berthomier, L. Fradette, J.R. Tavares, N. Virgilio, One-step processing of highly viscous multiple Pickering emulsions, J. Colloid Interface Sci. 560 (2020) 536-545.

[53] Y. Xue, X. Li, J. Dong, Interfacial characteristics of block copolymer micelles stabilized Pickering emulsion by confocal laser scanning microscopy, J. Colloid Interface Sci. 563 (2020) 33-41.

[54] L.L. Dai, S. Tarimala, C.Y. Wu, S. Guttula, J. Wu, The structure and dynamics of microparticles at Pickering emulsion interfaces, Scanning 30 (2008) 87-95.

[55] M. Kaganyuk, A. Mohraz, Role of particles in the rheology of solid-stabilized high internal phase emulsions, J. Colloid Interface Sci. 540 (2019) 197-206.

[56] M.C. Tatry, Y. Qiu, V. Lapeyre, P. Garrigue, V. Schmitt, V. Ravaine, Sugar-responsive Pickering emulsions mediated by switching hydrophobicity in microgels, J. Colloid Interface Sci. 561 (2020) 481-493.

[57] Y. Bao, Y. Zhang, P. Liu, J. Ma, W. Zhang, C. Liu, D. Simion, Novel fabrication of stable Pickering emulsion and latex by hollow silica nanoparticles, J. Colloid Interface Sci. 553 (2019) 83-90.

[58] J. Wang, H. Deng, Y. Sun, C. Yang, Montmorillonite and alginate co-stabilized biocompatible Pickering emulsions with multiple-stimulus tunable rheology, J. Colloid Interface Sci. 562 (2020) 529-539.

[59] C.E.P Silva, K.C. Tam, J.S. Bernardes, W. Loh, Double stabilization mechanism of O/W Pickering emulsions using cationic nanofibrillated cellulose, J. Colloid Interface Sci. 574 (2020) 207-216.

[60] C. Joseph, R. Savoire, C. Harscoat-Schiavo, D. Pintori, J. Monteil, F. Leal-Calderon, C. Faure, O/W Pickering emulsions stabilized by cocoa powder: Role of the emulsification process and of composition parameters, Food Res. Int. 116 (2019) 755-766.

[61] E. Tsabet, L. Fradette, Study of the properties of oil, particles, and water on particle adsorption dynamics at an oil/water interface using the colloidal probe technique, Chem. Eng. Res. Des. 109 (2016) 307-316.

[62] J.R. Lu, T.J. Su, R.K. Thomas, Structural conformation of bovine serum albumin layers at the air–water interface studied by neutron reflection, J. Colloid Interface Sci. 213 (1999) 426-437.

[63] M. Campana, S.L. Hosking, J.T. Petkov, I.M. Tucker, J.R.P. Webster, A. Zarbakhsh, J.R. Lu, Adsorption of bovine serum albumin (BSA) at the oil/water interface: A neutron reflection study, Langmuir 31 (2015) 5614–5622.

[64] J. Wang, H. Deng, Y. Sun, C. Yang, Montmorillonite and alginate co-stabilized biocompatible Pickering emulsions with multiple-stimulus tunable rheology, J. Colloid Interface Sci. 562 (2020) 529-539.

[65] V. N. Paunova, O. J. Cayreb, P. F. Noblea, S. D. Stoyanovc, K. P. Velikovc, M. Golding, Emulsions stabilised by food colloid particles: Role of particle adsorption and wettability at the liquid interface, J. Colloid Interface Sci. 312 (2007) 381–389.

Figures captions

Fig. 1. Microscopic images of W/O emulsions. Dispersed phase fraction of water of (a) ϕ = 0.10, (b) ϕ = 0.40, (c) ϕ = 0.50, and (d) ϕ = 0.75. Silica content ε = 1 wt.%, NaCl concentration λ = 1 wt.%.

Fig. 2. Droplet diameter distribution of W/O emulsions prepared at dispersed phase volume fractions (ϕ) of (a) 0.66, (b) 0.68, (c) 0.70 and (d) 0.75.

Fig. 3. Shear viscosity η and elastic modulus *G'* as a function of the dispersed-phase volume fraction ϕ. Comparison of the experimental viscosity data (points, triangles) with those calculated with the Pal approach (Eq. (4)) and those fitted by a power law expression (Eq. (6)). Comparison of the experimental elastic modulus (points, diamonds) with those fitted with the Princen model (Eq. (5)) and those fitted by a power law expression (Eq. (7)).

Fig. 4. Percolation model. Schematic representation of (a) the classical evolution of the viscosity at low shear rate (Newtonian plateau) η *vs* ϕ and G' *vs* ϕ when the percolation thresholds (ϕ_c (η) and ϕ_c (*G'*)) collapse. (b) Effect of the shear rate on the η *vs* ϕ curves.

Fig. 5. Comparison of experimental and percolation-model data of viscosity and elastic modulus as a function of the volume fraction of the dispersed phase. The percolation model was fitted to experimental data using Eqs. (8-9).

Fig. 6. Comparison of the elastic modulus of a Pickering emulsion ("Pickering") with those of surfactant-stabilized O/W (decane/water and kerosene/water) and W/O (water/dodecane) emulsions as a function of the dispersed-phase volume fraction (ϕ).

Fig. 7. Schematic representation of the possible modes of contact between the droplets for Pickering emulsions. (a) Particles network in the continuous phase. The particles are located in the interstitial fluid and form bridges between the droplets. (b) Particles adsorbed onto the droplets. (c) Coexistence of the 2 modes. (d) Droplet in the presence of multiple layers of solid particles (Nl = 3 layers) at the oil/water interface for the estimation of the effective volume fraction ϕ_{eff}.

Fig. 8. Comparison of the rheological properties of emulsions containing a disperse phase fraction of 0.75 in the presence of 1% by weight of silica (ϕ = 0.75, ε = 1%) with that prepared at 0.66 of disperse phase fraction and 2% by weight of silica (ϕ = 0.66, ε = 2%). Elastic modulus of reverse Pickering emulsions against shear strain for the two emulsions. The NaCl concentration (λ) is fixed to 1 wt.%.

GRAPHICAL ABSTRACT